Heterogeneity of Microscopic Congested Traffic Data Based on Drone Measurements

Yildirim Dülgar
Connected Navigation
Daimler AG
Sindelfingen, Germany
yildirim.duelgar@daimler.com

Michael Menth
Computer Science
University of Tübingen
Tübingen, Germany
menth@uni-tuebingen.de

Hubert Rehborn
Connected Navigation
Daimler AG
Sindelfingen, Germany
hubert.rehborn@daimler.com

Micha Koller
Cloud Applications Platform
Daimler AG
Sindelfingen, Germany
micha.koller@daimler.com

***Abstract*—We study vehicle trajectories at the onset and existence of traffic congestion and reveal its microscopic features on separate highway lanes. Drone observations of microscopic data of moving vehicles have been made available on three-lane road segments of German highways. Based on these detailed empirical traffic data we reveal heterogeneity and complexity of congested traffic and discuss its consequences. E.g., to perform a safe and comfortable driving behavior by driver assistance systems or automated vehicles lane-level traffic states should be adapted. A congested and dense traffic state only on the left lane of a three-lane highway could be a serious danger. Moreover, we propose an empirical method to calculate local traffic densities that could be used to warn vehicles in advance about high preceding densities. We leverage that concept to study a local traffic jam and discuss its lane-level properties. We reveal the heterogeneity of high local density structures on separate highway lanes.**

***Index Terms*—lane-level traffic, congested traffic, drone data, traffic analysis**

I. Introduction

The prevention of traffic accidents is a crucial topic for the traffic as a whole as well as for each individual driver. In this scope connected vehicles plays an important role. For example, upcoming congested traffic could be detected and shared by connected vehicles. The more vehicles are connected, the more precisely the upcoming congested traffic could be reconstructed. Lots of researches have been devoted to traffic warning systems and traffic reconstruction (see, e.g., [2], [3]). Common used traffic data for traffic reconstruction are *floating car data (FCD).* However, FCD only provide vehicle location points of a small amount of probe vehicles, e.g., 1% of the vehicles from the whole traffic. Therefore, a detailed analysis of all vehicle trajectories at a stretch of road over a certain time interval is not possible with FCD. Another important limitation of FCD is that traffic events, e.g., congested traffic, can not be reconstructed lane-specific. Congested traffic could occur differently on different lanes.

A complete and very precise measurement of all vehicle trajectories can be obtained through video recordings and aerial observations of a road segment, see Fig. 1 and Fig. 2. Lane-level vehicle positioning would be possible. With a *global navigation satellite system (GNSS)*, e.g., the *Global Positioning System (GPS)*, it is impossible to measure vehicle trajectories lane-specific due to the error of GNSS positions which could be up to 15 meters [4], [5]. Furthermore, with aerial observations we are able to calculate the *distance headway (DHW)* which is the distance between consecutive vehicles at a certain time instant. In Fig. 5 DHWs are symbolically marked at a certain time instant. Particularly for automated vehicles and advanced driving assistance systems (ADAS) both lane-level traffic information and density information could be very useful due to the complex traffic dynamics and the limitations of the vehicle sensors and the dynamic traffic states. In [6] empirical data are gathered by aerial observations with drones (*unmanned aerial vehicles (UAVs)*). By using the data we will investigate in this paper lane-level traffic structures and lane-level densities from DHWs. The data were measured during 2017 and 2018 on several German highways.

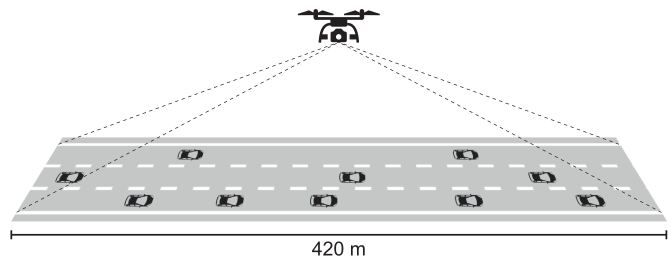

Fig. 1. A drone is recording a highway segment including all vehicle trajectories passing that segment at an altitude of more than 100 meters. A highway segment with a length of about 420 meters is covered.

The objective of this paper is the following. Using real comprehensive drone data measured on three-lane highway segments we reconstruct the traffic for each lane in space and time and compare the lane-level spatiotemporal traffic structures. We show the heterogeneity of the observed congested traffic structures and discuss its consequences, e.g., for automated or connected vehicles. Furthermore, based on distance headways between consecutive vehicles we reveal an empirical method that uses a moving average technique to calculate local traffic densities. We show and discuss the

Supported by the German Federal Ministry of Economic Affairs and Energy in the project *MEC-View* (FKZ: 19A16010B) [1].

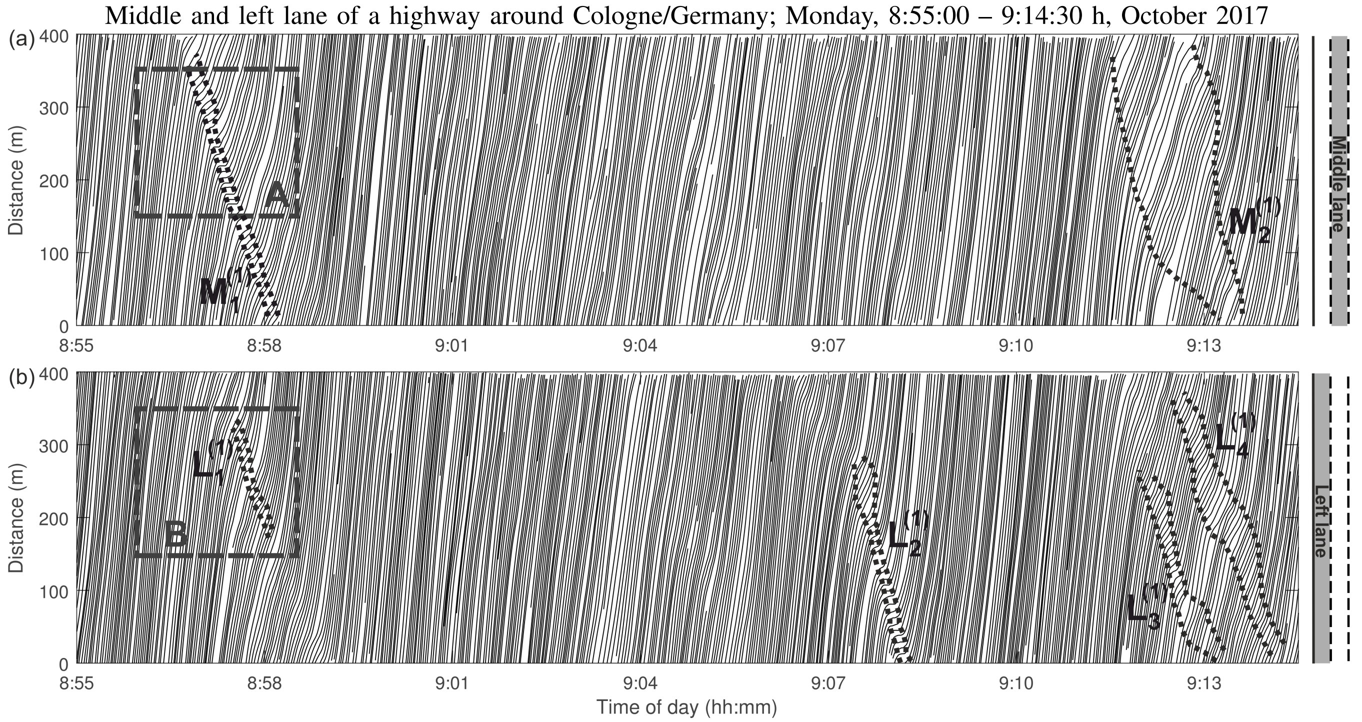

Fig. 2. Drone data from a German three-lane highway around Cologne at a Monday in October 2017 from 8:55:00 to 9:14:30 h. All vehicle trajectories from the middle (a) and left lane (b) are plotted over space and time as black lines. The black lines yield from connecting the vehicle front positions from each frame of the drone recording. The highway infrastructures are shown on the right of the distance-time plots. Congested traffic structures marked as $\mathrm{M}_1^{(1)}$, $\mathrm{M}_2^{(1)}$, $\mathrm{L}_1^{(1)}$, $\mathrm{L}_2^{(1)}$, $\mathrm{L}_3^{(1)}$ and $\mathrm{L}_4^{(1)}$ can be observed.

observed lane-level densities.

The paper is structured as follows. Section II gives a short overview about common used traffic data and the use of aerial observations to reconstruct traffic. In Section III the drone data used in this paper are described. In Section IV lane-level spatiotemportal congested traffic structures are discussed. Section V provides an empirical method based on lane-level local densities. Section VI concludes this paper.

II. Related Work

Through the availability of more comprehensive traffic data, more detailed vehicle attributes can be investigated, e.g., DHWs between consecutive vehicles. In [6] and [7] distributions of vehicle speeds and DHWs are studied based on empirical data from city traffic and highways. DHWs are not available if just FCD are used. Induction loop detectors make it possible to measure time headways (THWs) between consecutive vehicles, however, only at a certain location [8]. DHW and THW information are very useful for lane-changing. Lane-changing durations and dynamics have been studied in [7] and [9]. In [7] a detailed study about lane-changing durations and THWs have been done based on the empirical traffic data [10].

More than 40 years ago a comprehensive measurement of all vehicle trajectories passing a road segment has been done through aerial observations in [11] by Treiterer as well as in the project *Next Generation Simulation (NGSIM)* [10]. The NGSIM dataset was measured on highways and city traffic in the United States. In 2017 and 2018 city traffic was investigated by using drones in [12]–[14]. Recently, during 2017 and 2018 drone datasets have been recorded on German highways in [6] and will be used in this paper.

III. Drone Observations

In this paper, we will use empirical traffic data from drone observations measured during 2017 and 2018 on German highways around Cologne. The drone data is called *Highway Drone Dataset (highD dataset)* and inlcude $110\ 500$ different vehicle trajectories, $44\ 500$ driven kilometers and 147 driven hours [6]. The drone measurements have an average recording time of 17 minutes and cover a highway segment with a length of about 420 meters shown in Fig. 1. The drone data have been measured in altitudes of more than 100 meters and at six highway locations which are three- and two-lane highways. Since drones at altitudes of more than 100 meters are almost invisible for the drivers on the highway, it is assumed that the drones do not influence the driving behavior of the vehicles on the highway in any way. The positioning error of the measured vehicles on the highway are relatively small, generally less than ten centimeters [6]. In the drone data different traffic phases can be observed including congested traffic. This is very crucial for empirical traffic analysis purposes. For example in Fig. 2 (a) an upstream moving jams is observed between 8:56 and 8:58 h marked as

$M_1^{(1)}$. Since the highD dataset gives an unique opportunity to study real and detailed vehicle trajectories on highways, we will use the data for our empirical traffic investigations.

In Fig. 2 (a) and (b) a drone measurement from a German three-lane highway around Cologne with all vehicle trajectories from the middle and left lane are shown, respectively. The drone data was measured at a Monday in October 2017 from 8:55:00 to 9:14:30 h. The highway segment has a length of 400 meters and have been recorded over 19.5 minutes. The highway infrastructure is shown in Fig. 2 (a) and (b) on the right. The vehicle trajectories which are plotted as black lines in Fig. 2 (a) and (b) yield from connecting the vehicle front positions from each frame of the drone recording.

Fig. 3 (b) and (c) are subsets of Fig. 2 (a) and (b) marked by dashed squares A and B, respectively, between 150 and 350 meters and between 8:56:00 and 8:58:30 h. Each vehicle trajectory is plotted as a black line which yields from connecting the vehicle front position from each frame of the drone recording. The gray region along each vehicle trajectory in Fig. 3 shows the vehicle length. By considering the vehicle length large vehicles and trucks can be easily distinguished from passenger vehicles. For example, a truck can be observed in Fig. 3 (a) at 8:57:00 h and 150 m.

IV. Lane-Level Heterogeneity of Congested Traffic

By considering the vehicle trajectories from the drone observations for each lane in space and time various traffic structures can be observed. E.g., an upstream moving jam can be clearly observed in Fig. 3 (b) between 8:56:50 and 8:57:40 h marked as $M_1^{(1)}$. Particularly around this upstream moving jam $M_1^{(1)}$ the vehicle density is relatively high due to small DHWs between the consecutive vehicles. In Fig. 2 and Fig. 3 congested traffic structures are appearing for all three lanes at different time instants and highway locations. Some structures are appearing with an offset and a different spatiotemporal size on the other lanes, e.g., $R_1^{(1)}$, $M_1^{(1)}$ and $L_1^{(1)}$ in Fig. 3. Other structures are missing on the other lanes, e.g., $L_2^{(1)}$ in Fig. 2 or $R_2^{(1)}$ in Fig. 3 (a). Fig. 4 shows an empirical example of a congested and dense traffic state only on the left lane of a three-lane highway. In Fig. 4 the trajectories are colored according their speed values. On the left lane (Fig. 4 (c)) the traffic structures $L_2^{(2)}$ and $L_3^{(2)}$ can be observed between 17:26:45 and 17:29:00 h whereas on the middle and right lane (Fig. 4 (b) and (a), respectively) such structures cannot be observed. Fig. 4 emphasizes that empirical congested traffic structures appear lane-specific at different time instants and highway locations.

Moreover, we can observe that a vehicle has changed from the middle lane (Fig. 3 (b)) onto the left lane (Fig. 3 (c)) at 8:57:30 h and 160 m marked by black empty circles. The driver has changed the lane probably to avoid the upcoming jam on the middle lane marked as $M_1^{(1)}$ in Fig. 3 (b). On the left lane the upcoming jam marked as $L_1^{(1)}$ in Fig. 3 (c) appears later in space and time than on the middle lane. A

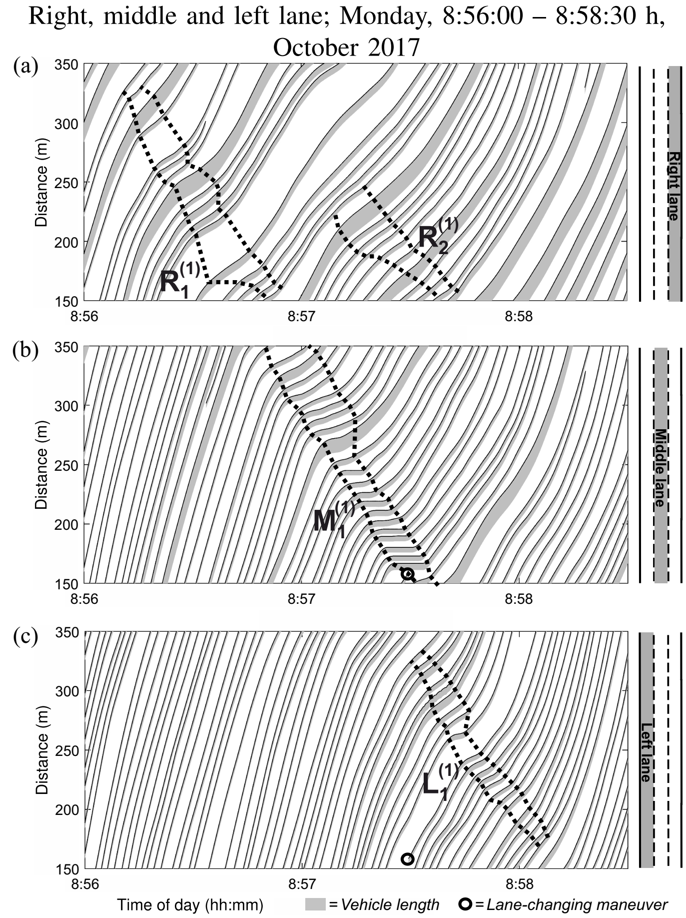

Fig. 3. Drone data from a German three-lane highway around Cologne at a Monday in October 2017 from 8:56:00 to 8:58:30 h. All vehicle trajectories from the right (a), middle (b) and left lane (c) are plotted over space and time as black lines. The black lines yield from connecting the vehicle front positions from each frame of the drone recording. The gray region along each vehicle trajectory shows the vehicle length. (b) and (c) are subsets of Fig. 2 (a) and (b) marked by gray dashed squares A and B, respectively. The highway infrastructures are shown on the right of the distance-time plots. The black empty circles show the position of the vehicles that have made a lane-changing. Congested traffic structures marked as $R_1^{(1)}$, $R_2^{(1)}$, $M_1^{(1)}$ and $L_1^{(1)}$ can be observed.

similar lane-changing maneuver can be observed in Fig. 4 (c) from the driver at 17:26:55 h and 70 m and from another driver at 17:27:20 h and 80 m marked by black empty circles. Both have changed the lane from the left lane onto the middle lane and, therefore, they are not entering the more congested traffic structure $L_2^{(2)}$. They probably changed the lane to avoid slower traffic on the left lane.

Congested traffic structures which appear only on one lane of a multiple-lane highway or appear at different time instants and highway locations could be a serious danger for automated vehicles and driver assistance systems. Therefore, the highway lane-level heterogeneity of congested traffic should be considered for these systems.

In the following section we will apply a moving average technique based on density information on the same data from Fig. 2 and Fig. 3 for each lane separately. It can also

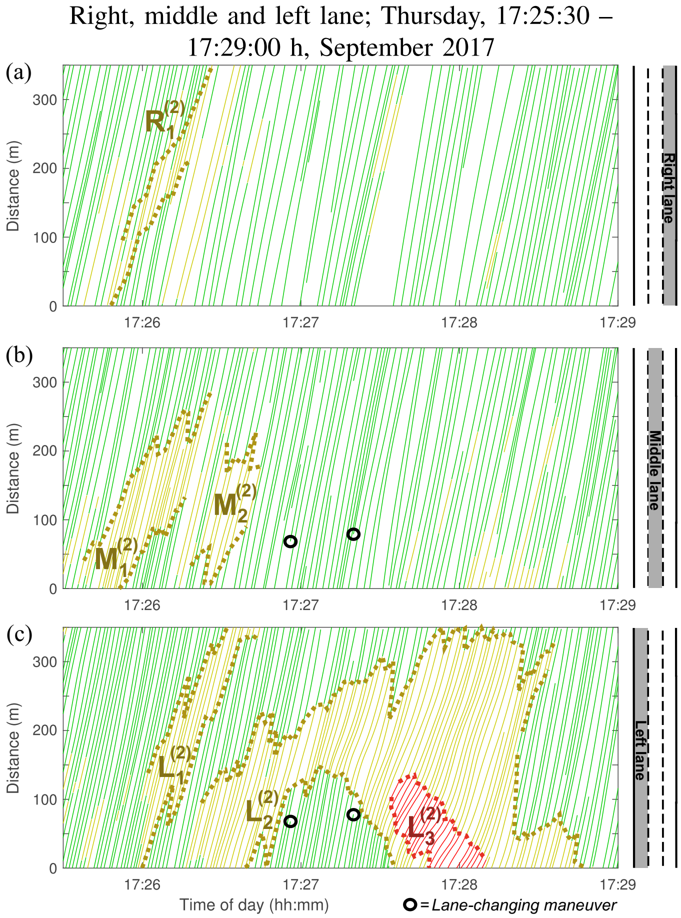

Fig. 4. Drone data from a German three-lane highway around Cologne at a Thursday in September 2017 from 17:25:30 to 17:29:00 h. All vehicle trajectories from the right (a), middle (b) and left lane (c) are plotted over space and time and are colored according the vehicle speeds as follows: red = 0–30 km/h, yellow = 30–60 km/h and green > 60 km/h. The black empty circles show the position of a vehicle that has made a lane-changing maneuver. The highway infrastructures are shown on the right of the distance-time plots. Congested traffic structures marked as $R_1^{(2)}$, $M_1^{(2)}$, $M_2^{(2)}$, $L_1^{(2)}$, $L_2^{(2)}$ and $L_3^{(2)}$ can be observed.

be observed in Fig. 7 that the calculated density structures appear at different time instants and highway locations. This observation is similar to the observations in Fig. 3 and Fig. 4.

V. Local Traffic Density: Moving Average Technique Applied to Distance Headways (DHWs)

In this section we propose a method that calculates local densities based on DHWs between consecutive vehicles. The method uses the moving average method *UTEMA* [15] and processes the empirical drone measurements [6]. We aim to apply the moving average method UTEMA to the DHWs for each frame of the drone recording. Especially for advanced driving assistance systems (ADAS) and automated vehicles density information calculated from averaged DHWs are important. The calculated density information could be used to warn vehicles in advance about high preceding local densities. Hence, the warned vehicles could react automatically or by the driver in adapting their driving behavior which would increase driving safety and decrease or even avoid congested traffic.

There are several studies devoted to unweighted, weighted and exponential moving averages, see, e.g., [16]. An *unbiased time-exponential moving average (UTEMA)* is proposed in [15]. Moving average methods are usually applied to ascending ordered time series. We aim to apply UTEMA to descending ordered location series instead of ascending ordered time series. Hence, an adaptation of UTEMA from [15] is needed. The procedure of the adapted UTEMA applied to location series is shown in Fig. 5 at a certain time instant. In Fig. 5 the vehicle at location d_{i+4} on the rightmost lane is symbolically getting the averaged density information $A_{d_{i+4}}$ from the preceding density information. The vehicle positions from one highway lane are defined as the location series $d_0, d_1, d_2, \ldots$ and measured by drones. X_{i+1} is the distance headway between the vehicles at the locations d_{i+1} and d_i. The average values $A_{d_0}, A_{d_1}, A_{d_2}, \ldots$ are calculated by the adapted moving average method UTEMA. We denote the average values A_{d_i}, which are calculated by applying UTEMA to DHWs, as *UTEMA-DHWs*. An important characterization of moving average properties is the metric *memory* M. The memory M is basically the space range over which the DHWs $X_0, X_1, X_2, \ldots$ are averaged. In Fig. 6 (c) and Fig. 7 we have used $M = 100$ meters.

Fig. 6 and Fig. 7 (b) are the subsets of the drone data in Fig. 2 (a) from 8:56:00 to 8:58:30 h and between 100 and 300 meters. Fig. 7 (c) is the subset of Fig. 2 (b) from 8:56:00 to 8:58:30 h and between 100 and 300 meters. In Fig. 6 (a) the vehicle trajectories are colored according their speeds, in Fig. 6 (b) according to the distance to preceding vehicles (DHWs) and in Fig. 6 (c) and Fig. 7 according to the averaged UTEMA-DHWs. An upstream moving jam within vehicles have usually very low speeds is marked by two dotted black lines in Fig. 6 (a). It can be observed that the vehicle speeds are higher before entering the upstream moving jam marked by orange colored trajectories with speeds between 20 and 35 km/h than after leaving the upstream moving jam marked by red colored trajectories with speeds between 0 and

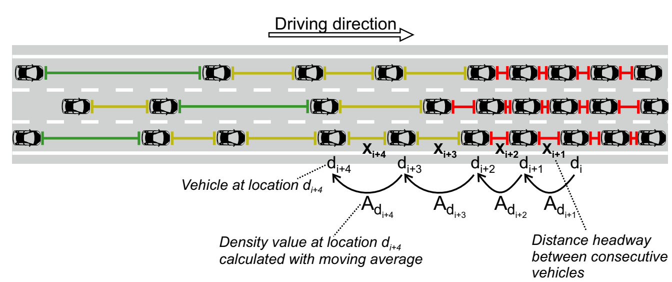

Fig. 5. At a certain time instant a frame of a drone measurement is symbolically shown. The distance headways (DHWs) $X_i, X_{i+1}, X_{i+2}, \ldots$ between consecutive vehicles are marked by lines in different colors: red for very small DHW, yellow for small DHW and green for little larger DHW. The procedure of UTEMA applied to descending ordered location series $d_i, d_{i+1}, d_{i+2}, \ldots$ at a certain time instant is shown. The density average values $A_{d_i}, A_{d_{i+1}}, A_{d_{i+2}}, \ldots$ (UTEMA-DHWs) are calculated by applying UTEMA to DHWs.

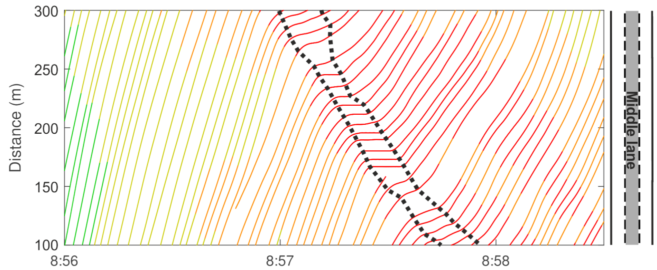

red = 0 – 20 km/h, orange = 20 – 35 km/h, yellow = 35 – 50 km/h, green > 50 km/h

(a) Vehicle speeds – middle lane

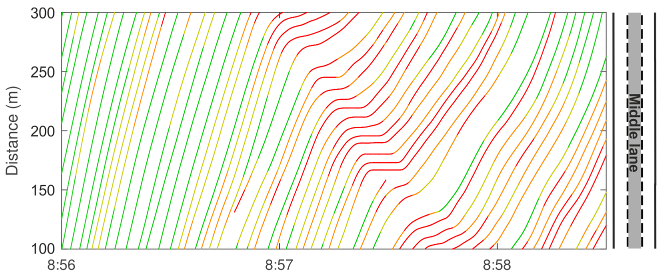

red = 0 – 10 m, orange = 10 – 15 m, yellow = 15 – 20 m, green > 20 m

(b) Distance to preceding vehicle (DHW) – middle lane

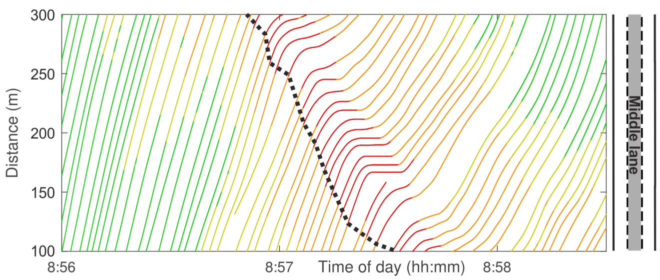

red = 0 – 10 m, orange = 10 – 15 m, yellow = 15 – 20 m, green > 20 m

(c) Averaged UTEMA-DHWs – middle lane

Fig. 6. All vehicle trajectories from the middle lane from the subset of Fig. 2 (a) from 8:56:00 to 8:58:30 h between 100 and 300 meters are shown. The vehicle trajectories in (a) are colored according the vehicle speeds, in (b) according the distance to preceding vehicles (DHWs) and in (c) according averaged UTEMA-DHWs. The color scales are shown below the distance-time plots.

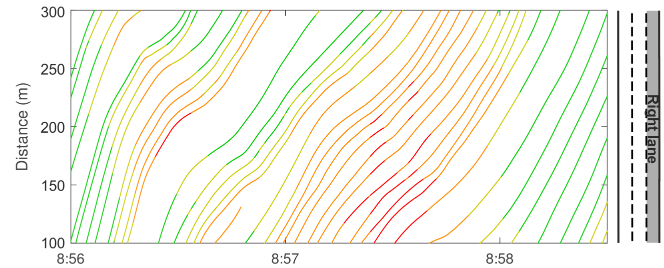

(a) Averaged UTEMA-DHWs – right lane

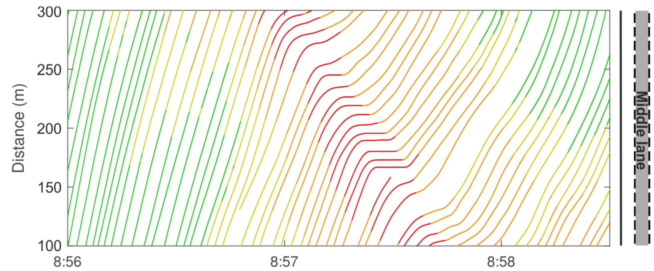

(b) Averaged UTEMA-DHWs – middle lane

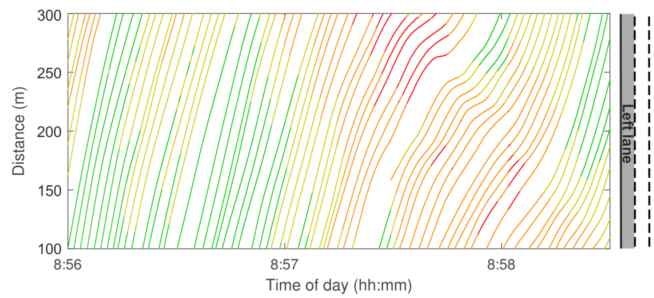

(c) Averaged UTEMA-DHWs – left lane

Fig. 7. All vehicle trajectories from the right (a), middle (b) and left lane (c) of a German three-lane highway around Cologne are shown. (b) and (c) are subsets of Fig. 2 (a) and (b), respectively, from 8:56:00 to 8:58:30 h between 100 and 300 meters. (b) is the same figure as Fig. 6 (c). The trajectories are colored according averaged UTEMA-DHWs as follows: red = 0–10 m, orange = 10–15 m, yellow = 15–20 m and green $>$ 20 m.

10 km/h. Moreover, we see in Fig. 6 (b) very small DHWs particularly inside the upstream moving jam. There are also vehicles after the upstream moving jam which are driving very closely to their preceding vehicles and have, therefore, very small DHWs marked by red colored trajectories with DHWs between 0 and 10 m in Fig. 6 (b).

We will have a closer look at Fig. 6 (c). A local density front marked by a dotted black line can be observed at the beginning of very low UTEMA-DHW values which are between 0 and 10 m. The density front is located in space and time before both the upstream moving jam which is marked by the two dotted black lines in Fig. 6 (a) and the very low DHW values marked in red in Fig. 6 (b). This is due to the definition of our local density method described above. Thus, the vehicles get the high density information (very low UTEMA-DHW values) before they reach the location at which vehicle speeds are very low and which is very dense (very low DHW values). Moreover, the density front has a similar upstream moving structure as the upstream moving jam marked in Fig. 6 (a). We note that the location of the density front in space and time depend on the memory used for the moving average method UTEMA.

Fig. 7 shows how the density information for each lane can differ from each other. As discussed above on the middle lane (Fig. 7 (b)) a local density front can be observed (marked in Fig. 6 (c) by a dotted black line) whereas on the right and left lane other density spots can be observed (in Fig. 7 (a) at 8:57:30 h between 100 and 150 m and in Fig. 7 (c) at 8:57:30 h between 240 and 300 m). Furthermore, it can be empirically observed that the calculated density structures in Fig. 7 appear at different time instants and highway locations and have a different spatiotemporal size. This is similar to the observations which have been made in Fig. 3 and Fig. 4.

VI. Conclusions and Outlook

Based on drone data we have shown the heterogeneity and complexity of lane-level congested traffic. We have analyzed and discussed two empirical examples: (i) Congested traffic structures are appearing for all three lanes at different time instants and highway locations. (ii) A congested and dense traffic structure is appearing only on the left lane of a three-lane highway. In both examples the spatiotemporal size of the congested traffic structures for each lane differ from each other. We have observed a similar lane-level behavior for high local densities. It is crucial that future technologies, e.g., new driver assistance systems, automated and connected vehicles, should consider and process lane-level traffic state information. This would increase driving safety and can give a more comfortable driving behavior.

Moreover, we have revealed an empirical method that uses a moving average method and calculates local densities based on distance headways (DHWs) between consecutive vehicles. The averaged density information could be used to warn a driver about upcoming high density or to give a driver a recommendation for lane-changing to avoid high upcoming traffic density on a specific lane.

A more detailed analysis of the microscopic structures of congested traffic could be performed based on the three-phase traffic theory [17] and more drone data sets at other complex infrastructures. The spatiotemporal drone measurements we have investigated show only some first interesting elements of traffic phase transitions. The spatiotemporal point at which a congested traffic structure starts, e.g., a moving jam, have not occurred in the observed road segments, but further downstream. The moving jam structure observed in the drone data is only a small snapshot of the overall complexity of traffic phases and its transitions.

Since the drone measurements give a detailed insight to real vehicle driving behavior on highways, they could be used to calibrate and improve traffic models. Such an investigation would be an interesting task for further studies.

Acknowledgment

We thank our partners for their support in the project *MEC-View* (FKZ: 19A16010B) [1], funded by the German Federal Ministry of Economic Affairs and Energy. We also thank the *Institute for Automotive Engineering (ika)* of *RWTH Aachen University* for providing highway drone data [6].

References

[1] (2017) Mobile edge computing based object detection for automated driving. Accessed December 18, 2018. [Online]. Available: http://www.mec-view.de

[2] B. S. Kerner, H. Rehborn, R.-P. Schäfer, S. L. Klenov, J. Palmer, S. Lorkowski, and N. Witte, "Traffic dynamics in empirical probe vehicle data studied with three-phase theory: Spatiotemporal reconstruction of traffic phases and generation of jam warning messages," *Physica A: Statistical Mechanics and its Applications*, vol. 392, no. 1, pp. 221–251, 2013.

[3] S.-E. Molzahn, H. Rehborn, and M. Koller, "Jam tail warnings based on vehicle probe data," *Transportation research procedia*, vol. 27, pp. 808–815, 2017.

[4] B. Hofmann-Wellenhof, H. Lichtenegger, and J. Collins, *Global positioning system: theory and practice*. Springer Science & Business Media, 2012.

[5] B. W. Parkinson, P. Enge, P. Axelrad, and J. J. Spilker Jr, *Global positioning system: Theory and applications, Volume II*. American Institute of Aeronautics and Astronautics, 1996.

[6] R. Krajewski, J. Bock, L. Kloeker, and L. Eckstein, "The highD dataset: A drone dataset of naturalistic vehicle trajectories on german highways for validation of highly automated driving systems," in *Proc. 2018 IEEE 21st International Conference on Intelligent Transportation Systems (ITSC)*, 2018.

[7] C. Thiemann, M. Treiber, and A. Kesting, "Estimating acceleration and lane-changing dynamics from next generation simulation trajectory data," *Transportation Research Record: Journal of the Transportation Research Board*, no. 2088, pp. 90–101, 2008.

[8] Y. Dülgar, H. Rehborn, S.-E. Molzahn, M. Koller, M. Menth, B. Kerner, and M. Schreckenberg, "A study for merging of automated vehicles," in *Proc. 27th Aachen Colloquium Automobile and Engine Technology 2018*, 2018.

[9] A. Kesting, M. Treiber, and D. Helbing, "General lane-changing model mobil for car-following models," *Transportation Research Record*, vol. 1999, no. 1, pp. 86–94, 2007.

[10] (2006) NGSIM - Next Generation Simulation. Accessed December 18, 2018. [Online]. Available: https://ops.fhwa.dot.gov/trafficanalysistools/ngsim.htm

[11] J. Treiterer, "Investigation of traffic dynamics by aerial photogrammetry techniques," Ohio State University, Columbus, OH United States, final report EES-278 Final Rpt., OHIO-DOT-09-75, FCP 40T2-052, PB 246 094, 1975.

[12] S. Kaufmann, B. S. Kerner, H. Rehborn, M. Koller, and S. L. Klenov, "Aerial observation of inner city traffic and analysis of microscopic data at traffic signals," *Transportation Research Board Annual Meeting*, 2017.

[13] S. Kaufmann, "Luftbeobachtung und Interpretation mikroskopischer Verkehrsmuster im übersättigten Verkehr vor Lichtsignalanlagen," Ph.D. dissertation, University of Tübingen, Germany, December 2018. [Online]. Available: http://dx.doi.org/10.15496/publikation-26626

[14] S. Kaufmann, B. S. Kerner, H. Rehborn, M. Koller, and S. L. Klenov, "Aerial observations of moving synchronized flow patterns in over-saturated city traffic," *Transportation research part C: emerging technologies*, vol. 86, pp. 393–406, 2018.

[15] M. Menth and F. Hauser, "On moving averages, histograms and time-dependent rates for online measurement," in *Proc. 8th ACM/SPEC on International Conference on Performance Engineering*. ACM, 2017, pp. 103–114.

[16] E. Zivot and J. Wang, "Vector autoregressive models for multivariate time series," *Modeling Financial Time Series with S-PLUS*, pp. 385–429, 2006.

[17] B. S. Kerner, *Breakdown in Traffic Networks: Fundamentals of Transportation Science*. Berlin: Springer, 2017.